ACCSCIENCE PUBLISHING

Materials Science in Additive Manufacturing

ORIGINAL RESEARCH ARTICLE

# Development of a compact multi-material vat photopolymerization printing solution

**Wudith W. Niyagama*, S. Siddharth Kumar, Tuomas Puttonen, and Jouni Partanen**

Department of Energy and Mechanical Engineering, Aalto University, Espoo, Finland

## Abstract

Multi-material vat photopolymerization (MMVPP) is an emerging additive manufacturing technology with great potential in biomedical engineering, soft robotics, electronics, and customized manufacturing, particularly where functional gradients and spatially varying material properties are essential. The capability to precisely control composition at the voxel level enables the fabrication of bioinspired structures and multifunctional components with tailored mechanical and functional performance. This study presents the conceptual design and development of a compact and commercially viable MMVPP system that addresses key challenges in current state-of-the-art technologies. A two-vat prototype printer was fabricated to demonstrate the feasibility of precise multi-material printing. Critical challenges, including resin compatibility, interfacial adhesion, and mechanical property optimization, were systematically investigated. Novel strategies such as variable layer height exposure control, overlapped layer printing, and optimized curing parameters were introduced to improve interfacial bonding and overall structural integrity. The proposed methods were validated through mechanical testing, confirming enhanced interface strength and material cohesion. The study also details system-level innovations, including efficient vat-switching mechanisms and process synchronization for rapid material transition. These advances establish foundational methodologies for reliable multi-material photopolymerization and expand the design space of photopolymer-based additive manufacturing. The results demonstrate MMVPP's transformative potential to enable next-generation manufacturing of functionally graded and multi-material components with superior performance and design freedom.

***Keywords:*** Process design; Vat photopolymerization; Photopolymer resins; Digital light processing; Multi-material interface evaluation; Additive manufacturing

***Corresponding author:**
Wudith W. Niyagama
(wudith.niyagamagamage@aalto.fi)

**Citation:** Niyagama WW, Kumar SS, Puttonen T, Partanen J. Development of a compact multi-material vat photopolymerization printing solution. *Mater Sci Add Manuf*. 2026;5(2):025510122. doi: 10.36922/MSAM025510122

**Received:** October 29, 2025

**Revised:** December 19, 2025

**Accepted:** December 26, 2025

**Published online:** February 27, 2026



## 1. Introduction

Additive manufacturing (AM), with its layer-by-layer fabrication approach, offers a diverse range of possibilities in modern manufacturing by enabling complex geometries, reducing material waste, and allowing rapid prototyping and customization.[1] Multi-material AM extends these capabilities by combining different materials within a single print. This enables the development of advanced composites such as functionally graded materials[2] and supports complex applications including soft robotics, multifunctional

sensors, and bioengineered implants,[3-6] significantly enhancing the overall functionality of manufactured components. Moreover, multi-material AM facilitates the fabrication of smart programmable composites through innovative 4D printing approaches that can change shape or properties over time in response to external stimuli such as heat, light, electric, magnetic, or moisture.[7,8]

Among the seven AM processes recognized by the International Standards Organization/American Society for Testing and Materials (ISO/ASTM) standard (ISO/ASTM 52900:2021), not all are equally suited for multi-material fabrication. Technologies relying on sequential or spatially controlled deposition of photopolymers offer distinct advantages, as they allow rapid switching between materials and enable high-resolution patterning of dissimilar chemistries within a single build vat photopolymerization (VPP) uses a light source to selectively cure photopolymer liquid resin layer by layer within a vat, creating intricate and high-resolution parts through technologies such as stereolithography (SLA) and digital light projection (DLP). Material jet printing (MJT), on the other hand, involves the precise deposition of material droplets onto a build platform using print heads to form objects layer by layer, allowing for detailed multicolor and complex geometries.[1] Both technologies have demonstrated strong potential for multi-material AM due to their precise voxel-level control, compatibility with a wide range of functional resins, and ability to fabricate parts with sharp material interfaces.[9] For these reasons, photopolymer-based technologies such as VPP and MJT provide high-resolution manufacturing capabilities.[1] MJT has evolved with multi-material capability and can achieve layer thicknesses as low as 0.013 mm. Currently, the resolution of material jetting can reach up to 5000 × 5000 dots per inch (DPI) in the horizontal plane (AMpolar® i2, ALTANA AG, Germany).

VPP technology has evolved into different variants based on the curing approach. Most prominently, SLA and DLP are widely used in both commercial and research applications.[10] SLA uses a laser to selectively cure a photopolymer resin layer by layer on a build plate, whereas DLP systems utilize a projected ultraviolet (UV) light source instead. The resolution of SLA systems can reach up to 4000 DPI, with a minimum layer thickness of 0.03 mm. DLP systems, such as masked projection VPP, can achieve resolutions of 25 μm and layer thicknesses of 25 μm.

Moreover, resin viscosity is a key factor. MJT printing typically accommodates inks with viscosities around 150 cP or lower, where the resin is heated up to 60°C at the printhead to reduce viscosity to approximately 20 cP.[11] In contrast, the viscosity of resins used in VPP can reach up to 5000 cP. The primary limitation on viscosity in VPP arises from the need for the resin to self-level in the vat as quickly as possible to prepare for the next curing layer.[12]

Many researchers have attempted to develop multi-material VPP (MMVPP) systems using different techniques and unique setup configurations. MMVPP was pioneered by Wicker's group[13-15] in 2004 with the earliest known vat-switching mechanism. Their system employed a rotary vat carousel capable of switching vats in the horizontal plane. The build plate, fixed to the rotary platform, had a horizontal axis of rotation that enabled manual cleaning. The printed part was cured using a numerically controlled laser placed above the vat. Hence, they adopted an overhead curing method that required a floating target to maintain precise resin levels, as the platform needed to be positioned at an exact depth to enable the overhead curing process. This configuration required a significantly larger amount of resin compared to the bottom-curing method, which does not require submerging the entire build platform.

Chen's group[16,17] worked on image-based SLA, where they implemented a rotary-based vat carousel system for switching between vats and cleaning stations. Their setup incorporated a cleaning mechanism during material switching, consisting of an ultrasonic cleaner, two brushes, and an air-blowing station used to clean the build platform. They adopted a bottom-curing method. Similarly, Bhusal *et al.*[18] developed a bottom-up printing method in which curing was performed using a UV source from below. Masking of the UV light was achieved with a gel-based commercial orange food dye. Vat switching was accomplished using a rotary platform, whereas the cleaning process involved dipping the build plate in a phosphate-buffered saline solution. The system was customized for the fabrication of hydrogel-based microfluidic chips.

Jiang *et al.*[19] advanced MMVPP technology for developing soft robotic grippers. They adopted a rotary vat carousel system with three vats and a cleaning station equipped with air and alcohol spray nozzles. The uniqueness of this setup lies in combining both cleaning and drying functions within a single position, thereby saving space and reducing translation time.

Matte *et al.*[20] proposed a unique vertical vat storage system in which vats are extracted horizontally from a tower to a curing station. The design incorporated a combined cleaning approach, where brush heads were fixed inside each vat to remove resin droplets adhered to the build surfaces. The system also featured an active cleaning mechanism using a sprinkler system that sprayed solvent onto the build platform while the platform moved along three axes relative to the nozzles.

Shaukat *et al.*[21] and Ghaderi *et al.*[9] presented similar MMVPP setups featuring two vats and a cleaning station arranged in a linear configuration, with the cleaning station positioned between the vats. Shaukat's system used a sponge to clean the build and platform, whereas Ghaderi's employed an ultrasonic cleaning system. In both configurations, all three stations moved horizontally, whereas the build plate moved vertically. Khatri *et al.*[22] proposed a linear vat-switching approach in which the build plate moved along the vertical axis, whereas the vats were exchanged along the horizontal axis. The system included a UV projector and a resin-handling mechanism to support multi-material capability.

Hu *et al.*[23] developed a similar DLP system featuring three vats in a linear configuration. The build platform was lowered during printing while the UV image was projected from the bottom of the vat. When switching vats, both the build platform and the projector moved linearly from one vat to another. Independent drying and cleaning stations were also incorporated, with the cleaning station equipped with nozzles that sprayed a surfactant solution.

Cheng *et al.*[24] also adopted a similar linear-configuration MMVPP system; however, the uniqueness of their setup lies in the cleaning system used during resin switching. When the build platform lifts off the resin bath after curing a layer, it spins at 10,000 rpm, causing residual resin to be flung off through centrifugal force. This eliminates the need for physical wiping or the use of active automated cleaning methods involving liquid cleaners such as isopropyl alcohol.

Prior research on MMVPP has employed a range of strategies to address vat switching, cleaning, drying, and related process steps. From these studies, the principal challenges associated with MMVPP implementation can be identified, leading to the following key observations.

Placing the vats in a vertical tower configuration[9] presents challenges, as extraction from the storage tower involves a significant number of moving parts and occupies considerable unused space. Moreover, an excessive number of moving components or mechanisms dedicated solely to vat switching may cause reliability issues.

In contrast, having vats arranged linearly,[10,11] where the build plate moves along the axis parallel to the vat placement, allows a cleaning station to be positioned between them. However, due to cross-contamination concerns, the number of materials that can be used simultaneously is typically limited to two. This configuration also requires separate curing setups for each vat. Allowing the build plate to drip off excess resin while idling above the current vat, such as in Hu *et al.*'s setup,[23] can reduce cross-contamination and minimize material wastage, although it significantly increases process time.

The main drawback of rotary carousel systems, such as those developed by Wicker and Chen, is that the carousel diameter increases with each additional material. Although this approach requires only one curing station, it occupies a larger overall volume, making it difficult to scale down to a compact, desktop-level system.[13,16]

An automated cleaning mechanism during material (vat) switching has become essential to replace manual cleaning. Cleaning techniques such as sponge wiping[22] and centrifugal cleaning[24] do not ensure uniform removal of uncured resin from complex geometries. It has been demonstrated that ultrasonic cleaning is highly effective in MMVPP applications, as solvents such as isopropyl alcohol can clean build surfaces regardless of their geometry.[16] Moreover, Ghaderi *et al.*[9] investigated resin cross-contamination in MMVPP systems and achieved 100% cleaning efficiency when ultrasonic cleaning was employed.

Many of the above researchers have conducted experiments to demonstrate the printing capabilities and specific techniques developed to overcome challenges during the process. Ghaderi *et al.*[9] performed multi-material printing tests using various geometries, where clear boundaries were observed between materials, whereas Zhou *et al.*[16] produced samples with mixed matrices, resulting in isotropic material properties.

Several studies[9,21,24] have also conducted mechanical testing of MMVPP-printed specimens to evaluate the mechanical performance of multi-material interfaces. Shaukat's experiments revealed that two-material samples exhibited significantly lower tensile strength compared to single-material samples.[21] Ghaderi *et al.*'s work included compression testing on cubic samples with different interfacial angles to study the effect of interface geometry on mechanical performance.[9] Based on the above literature, the key elements to consider when developing a multi-material system are curing geometry, vat configuration, and cleaning technique.

This study, therefore, aims to investigate the critical design considerations and practical hardware requirements for developing a compact and commercially viable MMVPP system. It further seeks to identify key challenges and inherent limitations of MMVPP technology and to explore effective strategies for overcoming these issues to optimize print quality. In addition, the research examines the mechanical performance of multi-material specimens, with particular emphasis on assessing how the interface quality between different materials compares to that of single-material specimens.

## 2. Methods

Based on the findings from the state-of-the-art MMVPP systems, the aim of this study is to conceptualize a design that accommodates multiple material vats while allowing the number of vats to be scaled up without major modifications to the overall system architecture. Moreover, the methods of cleaning and drying between material switches are crucial, as effective cleaning techniques must achieve zero cross-contamination between different resins while minimizing process time. Table 1 summarizes the objectives of this study and the sub-sections where the corresponding methods are used.

### 2.1. System conceptualization

This section describes the conceptual design of an MMVPP system incorporating key elements such as vat placement, build plate movement relative to the vats, and the integration of cleaning and drying stations.

Figure 1 illustrates the initial design concept of an MMVPP setup consisting of nine vats arranged in a 3 × 3 configuration and an adjacent cleaning station. The model was created using SolidWorks (v2024, Dassault Systèmes SOLIDWORKS Corp., Waltham, USA). The vat array dimensions are denoted as $l_x$ and $l_y$ in the X and Y directions, respectively. The build platform motion is constrained to two-thirds of $l_x$ and to $l_y$ in the horizontal (X–Y) plane, indicated by red and green arrows, respectively. Vertical motion typical in conventional VPP systems is represented by blue arrows.

The vat dimensions are designed such that $l_x > l_y$ to enable the use of commercially available monochrome displays, as this system relies on an LCD-type VPP process.

**Table 1. Research objectives and method sections**

| No. | Objectives | Method sections |
|---|---|---|
| 1 | To develop a concept of commercially viable MMVPP technology | 2.1. System conceptualization |
| | To demonstrate the working concepts through a proof-of-concept prototype | 2.2. Prototype development |
| 2 | To systematically identify the practical limitations of printing with MMVPP technology and implement solutions to address them | 2.3. Multi-material experiment: Material boundary between distinct layers |
| | | 2.4. Intra-layer multi-material exposure control |
| 3 | To evaluate the multi-material interface and compare its mechanical properties with single-material specimens | 2.5. Testing for mechanical properties at the interface |

The vats are proportioned so that all nine can be selectively projected using a single UV light source and masking display, eliminating the need for multiple light sources or displays. Each vat is relatively shallow (approximately 8 mm) compared with conventional systems. For example, a 154 mm masking display with a pixel density of 1500 DPI (equivalent to 0.017 mm horizontal resolution) provides sufficient precision for each vat in the 3 × 3 grid.

A bottom-curing configuration with a transparent vat base allows the structure to be built inverted, attached to the underside of the build platform. The vat bottom must therefore be optically transparent. During printing, the build plate is lowered to create a gap equal to the desired layer height. Since most layer heights are below the sub-millimeter range, the resin level can be maintained below 3 mm, which minimizes resin consumption and reduces contamination of the build plate. Compared with top-curing setups, bottom-curing offers significant advantages in system compactness and in reducing contamination of both the build plate and printed part.

To remove uncured resin from the build and platform during vat switching, an automated cleaning system is essential. Previous studies have demonstrated the effectiveness of ultrasonic cleaning in MMVPP applications.[13,16,25]

As shown in Figure 2, the cleaning station is positioned adjacent to the vat array along the X-axis to maintain system compactness. It consists of a container equipped with an ultrasonic transducer at the bottom. The cleaning tray is deeper than the vats so that the build plate and part can be fully submerged. When submerged, the transducer generates high-frequency waves within an alcohol bath, dissolving and dislodging residual resin. The ultrasonic cleaning station shares the same horizontal dimensions as a vat, ensuring compatibility with the motion path and maintaining minimal contamination during layer-by-layer processing.

Figure 1 also indicates another vital component, the air-blowing unit (black arrows). Although ultrasonic cleaning effectively removes uncured resin, it may leave behind residual solvent (isopropyl alcohol), which can impair interlayer adhesion.[16] Cleaning of photopolymer resins typically uses isopropyl alcohol at concentrations above 90%,[26] and at such concentrations, isopropyl alcohol is highly volatile.[27] Therefore, a blow-drying operation is introduced to remove residual solvent from the build surface and platform.

As illustrated in Figure 3, the blowing station incorporates two air-blowing units that direct a stream of air through nozzles onto the build surface to evaporate

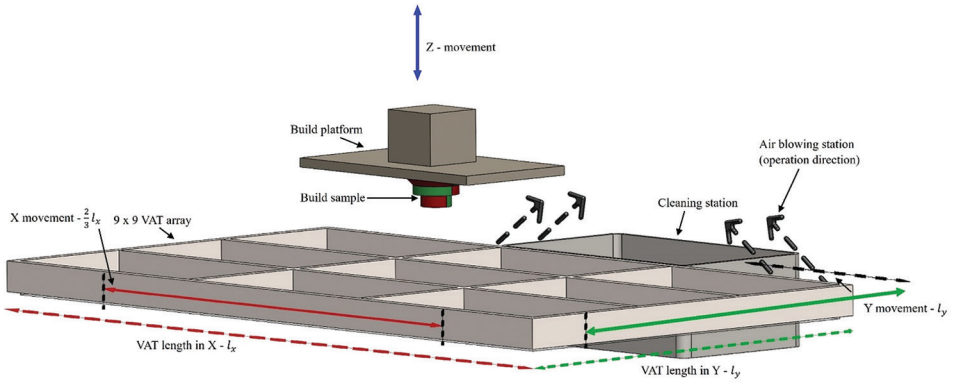


**Figure 1.** Schematic of a multi-material vat photopolymerization system

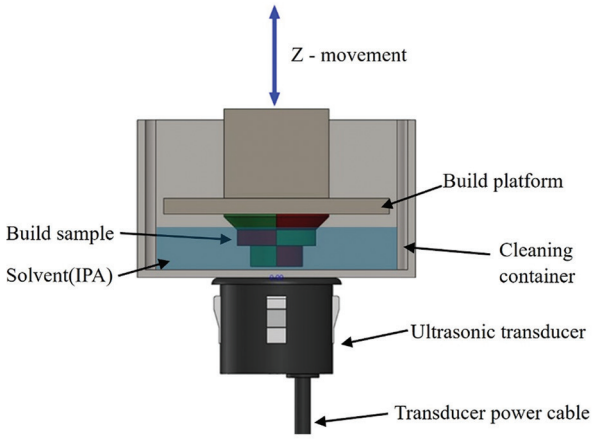


**Figure 2.** Schematic of cleaning station (sectional view)
Abbreviation: IPA: Isopropyl alcohol

excess cleaning solution. After ultrasonic cleaning, the build platform is raised to a hold position above the cleaning tray and allowed to drip for approximately 5 s. Subsequently, the air-blowing units operate to dry any remaining isopropyl alcohol from the build surface and platform. This step prevents solvent contamination between the cleaning and printing stages. Placing the cleaning and drying stations vertically—one above the other—eliminates the need for separate stations, resulting in a more compact and integrated design.

## 2.2. Prototype development

Building upon the conceptual framework of the MMVPP system, which outlined the principles for achieving multi-material with a multi-vat design as well as resin switching and coordinated photopolymerization, the next stage focused on translating these ideas into a tangible prototype. The conceptual design served as a blueprint, guiding key engineering decisions related to resin handling, optical alignment, and mechanical integration. Emphasis was placed on realizing the core functionalities that would validate the feasibility of the concept, particularly the mechanisms enabling material switching and localized curing. This transition from conceptualization to prototyping aimed to identify the practical challenges, such as resin level control, material cross-contamination, and synchronization of exposure processes, that must be addressed to fully implement the envisioned MMVPP platform.

Figure 4 shows the test setup developed to demonstrate a two-material VPP. The prototype was built by modifying a Creality Halot One printer (Creality 3D Technology Co., China), a DLP-based VPP system. The original printer provides a print volume of 127 × 80 × 160 mm$^3$, with 402 nm UV light masking enabled through a monochrome display offering a resolution of 0.01–0.05 mm in the XY plane.

To enable multi-material capability, the commercial printer was modified by adding a horizontal motion axis. A stepper motor drives a leadscrew mechanism, providing linear motion of the build platform along a linear guide rail to maintain motion precision. This additional axis is mounted asymmetrically to compensate for the motor's weight.

The development of a new vat system presented challenges, as switching vats to change materials can lead to cross-contamination between resins. Reducing the resin volume in each vat, therefore, minimizes the risk of contamination. In addition, a lower vat height further contributes to this objective by limiting residual resin and facilitating more efficient material exchange. The build plate has an active area of 44 × 75 mm, whereas the vat system consists of two vat trays, each measuring 75 × 96 × 16 mm. The overall dimensions of the assembled setup are 262 × 221 × 404 mm.

The original control circuit board contained proprietary technology, which was protected from modification and

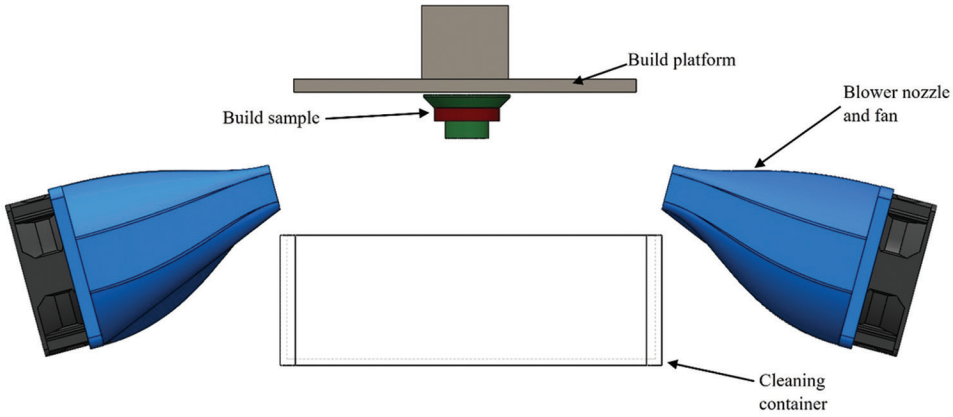


**Figure 3.** Schematic of the air blowing station

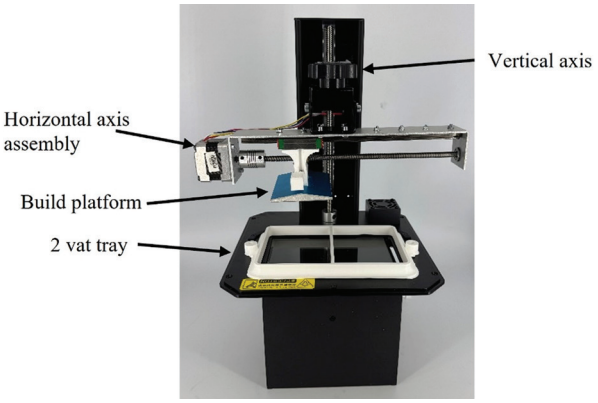


**Figure 4.** Prototype two-material vat photopolymerization system

was replaced with a new control setup. A Raspberry Pi 4 model B (Raspberry Pi Ltd, Cambridge, England) is utilized as the controller, along with two stepper motor drives that are utilized to control the horizontal and vertical stepper motors. A limit switch defines the home position, and the bottommost position is determined relative to this reference. The control system schematic is provided in the Appendix. For this prototype, a manual cleaning mechanism was implemented to validate the core printing functions, serving as a precursor to future integration of an automated ultrasonic cleaning system.

Compared with a nominal LED-based DLP system, the main alignment challenge arises because the masking image must be projected at two distinct locations rather than a single fixed position, enabling the curing of two different photopolymer resins. Consequently, it is critical to precisely align each masked image with the corresponding region of the build platform during every curing step. This coordination is achieved through synchronized control of the build plate's horizontal actuation and the masking sequence of the LED display.

### 2.3. Multi-material experiment: Material boundary between distinct layers

In MMVPP printing, one of the key elements demonstrates and evaluates the resin switching. To better understand the process and the parameters related to switching of resins, a sample was modeled with unique features. Different exposure parameters, such as exposure time, build plate lifting height, and layer thickness, were varied to determine optimal values and to assess overall printing performance.

To establish suitable printing parameters, a commercial Anycubic Standard photopolymer clear resin was used together with a cyan, magenta, yellow, and black pigment set supplied by Primacreator (Prima Printer Nordic AB, Malmö, Sweden). Pigments were mixed into the clear resin to create colored formulations, which were used to emulate different materials.

Initially, a series of single-color benchmark samples (Figure 5A) was printed to validate baseline parameters. Each sample measured 10 mm in height and was printed with a 0.05 mm layer thickness over 100 layers. In the multi-color tests (Figure 5B), the lower 50% of layers were printed using one colored resin, followed by the remaining layers in a different color to simulate inter-layer material transition. All samples were printed with an initial exposure of 40 s followed by a layer exposure of 3 s. The motor speed was set to 3 mm/s.

Sample heights were measured using a micrometer screw gauge with a precision of ±0.01 mm. Measurements were taken at three points along the vertical axis, and the mean value was recorded to minimize measurement error.

The primary objective of this experiment was to evaluate the effect of layer thickness variation on the overall printed height of two-color specimens fabricated using the dual-material VPP system. The layer thickness was

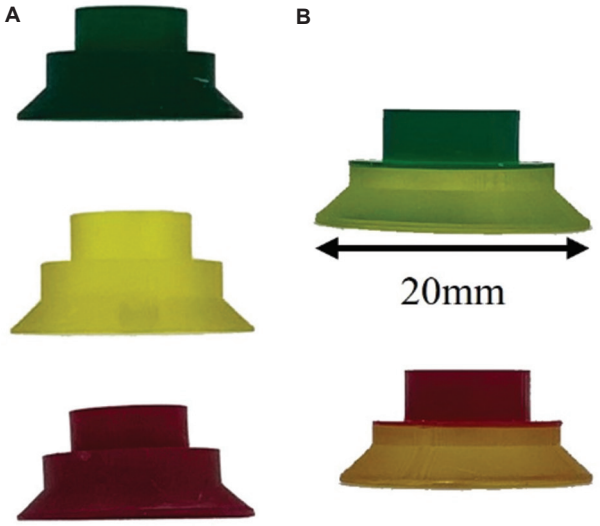


**Figure 5.** Resin-printed samples. (A) Single-color sample; (B) Multi-color sample

systematically varied between 0.035 mm and 0.100 mm while maintaining consistent exposure time, resin viscosity, and environmental conditions. This approach isolated the effect of layer thickness on dimensional accuracy.

### 2.4. Intra-layer multi-material exposure control

MMVPP presents unique challenges during intra-layer curing, where two materials are processed sequentially within the same layer. After the first material is cured, the build plate is raised to allow vat switching. The used vat is replaced with one containing the second material and then lowered back to the original z-position to cure the second material in the same layer. However, when the previously cured region comes into contact with the vat bottom, a thin layer of uncured resin from the second material remains beneath it. This creates a slight positive z-error, where the distance between the build plate and the vat bottom becomes greater than intended. Consequently, the second material forms a thicker layer than the first, resulting in a stepwise height error. Over successive layers, these discrepancies accumulate, leading to dimensional inaccuracies. Furthermore, because curing parameters are optimized for thinner layers, the thicker regions receive insufficient UV exposure, leaving the material partially uncured.

#### *2.4.1. Layer offsetting*

To mitigate this error, the print sequence was modified, as shown in Figure 6. The build plate is lowered to create a gap of the intended layer height ($h$ mm) between the build surface and the vat bottom containing Material 1 (red). The resin is then exposed and cured. After curing, Material 1 is cleaned in the cleaning station (Figure 6B), and the build plate is lowered to a position $2h$ mm above the vat bottom

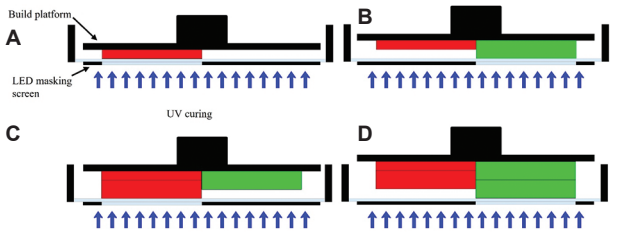


**Figure 6.** (A-D) Schematic of printing two materials with variable layer height

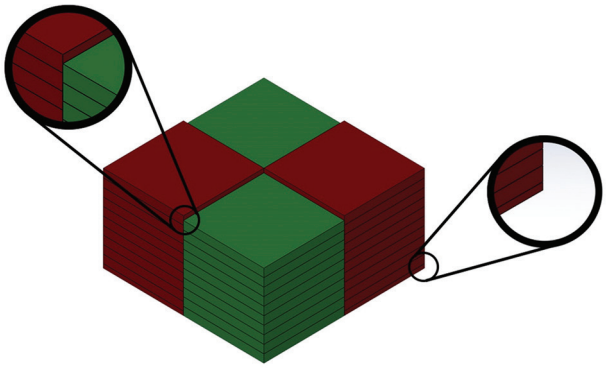

**Figure 7.** Sample of two materials printed with different layer levels

of Material 2 (green). This adjustment ensures that a gap of $h$ mm exists between the vat bottom and the already cured region of Material 1, preventing contact and potential damage to the masking display or vat film.

As shown in Figure 6C and D, each subsequent layer is cured with an offset of $h$ mm relative to the previous one. The resulting offset between the two materials in the final layer defines the process resolution, as it corresponds to the minimum step height achievable through this sequential curing approach.

This method can be extended to a full multi-material scenario, as illustrated in Figure 7, where a sample with four distinct two-color sections was fabricated. Printing began with red resin at an initial layer height of 0.05 mm, followed by green resin with a layer height of $2h$ mm. The printing sequence alternated between the two colors, maintaining an offset of $h$ mm between layers until completion. Offsets of this magnitude are typical in AM processes and are generally negligible compared to the overall part dimensions.[28]

#### *2.4.2. Layer offsetting with overlapping*

Although varying layer heights for different materials (as in Figure 6) improves process stability, it produces a sharp vertical interface between the two resins. Such interfaces may lead to weak bonding. Possible causes include minor misalignment of the build plate or the

partial removal of uncured resin during cleaning—whether manual or ultrasonic—which reduces interfacial adhesion.

To address this, an overlapped exposure strategy was implemented, as shown in Figure 8. In this schematic, black regions of the LED display represent masked areas, where the light blue (transparent) regions correspond to UV-exposed zones. First, a 0.05 mm layer of red resin was cured (Figure 8A), followed by a 0.1 mm layer of green resin (Figure 8B). The green resin overlapped the red region by 3 mm, resulting in an overlapped curing height of 0.05 mm. This step was then repeated with reversed colors (Figure 8C), allowing red resin to overlap onto the green region.

This approach significantly strengthens the interfacial bond between the two materials because the effective bonding area increases. The overlap introduces both vertical and horizontal contact surfaces, whereas non-overlapped boundaries (as in Figures 3A and 7A) produce only vertical interfaces.

The experimental validation is shown in Figure 9, which demonstrates MMVPP within the same layer. Both samples (as in Figure 9A and B) consisted of 20 layers, each 0.1 mm thick, printed using two colored resins. In Figure 9A, a distinct boundary is visible between materials, corresponding to the non-overlapped printing method illustrated in Figure 6. In contrast, the sample in Figure 9B was printed using the overlapped exposure approach from Figure 8, with a 3 mm overlap region. Both samples were 2 mm thick; however, the non-overlapped sample (Figure 9A) exhibited cracking at the material interface, whereas the overlapped sample (Figure 9B) maintained structural integrity. These results demonstrate the improved interfacial bonding achieved through overlapped intra-layer exposure, validating the feasibility of multi-material printing with both layer offset and material overlap strategies.

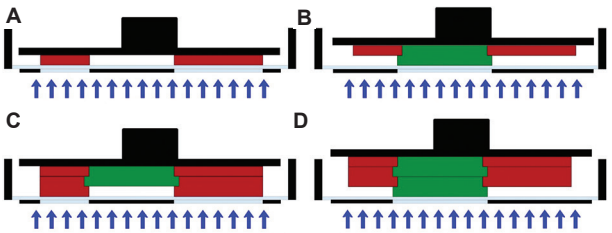


**Figure 8.** (A-D) Schematic of printing two materials with variable layer height, with overlapping

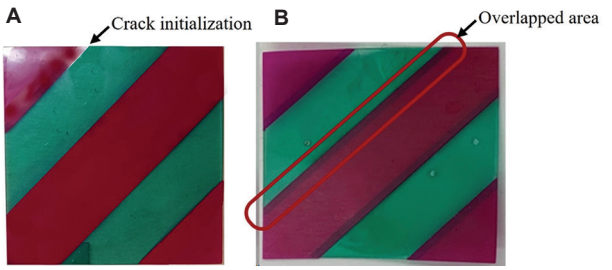


**Figure 9.** Multi-material printed sample in the same layer. (A) Non-overlapped; (B) Overlapped

## 2.5. Testing for mechanical properties at the interface

To validate the printing methodology and assess the mechanical properties of the fabricated specimens (as shown in Figure 10), a series of tensile tests was conducted. The test specimens were modeled according to the ASTM D638–22 standard for tensile testing.[29]

Samples were printed in three categories—monolithic, no-overlap, and overlap—with three specimens per category. Monolithic samples made from a single material were used as reference specimens. Each sample measured 63.5 × 9.53 × 0.5 mm$^3$. The multi-material samples were printed using two differently pigmented resins, consistent with those described in section 2.5 and shown in Figure 10A. One set of multi-material specimens incorporated an overlap (y = 1 mm) following the printing method illustrated in Figure 8, while the other set was printed without overlap (y = 0). Tensile testing was performed using an MTS Insight™ electromechanical tensile testing machine.

To ensure adequate gripping during testing, 4 mm spacers were attached to both ends of the specimens, as shown in Figure 10B. These spacers were fabricated from the same resin. They were manually attached and UV-cured at the interface surfaces to improve fixture alignment. Due to the brittle nature of the UV-cured resin material,[30,31] the crosshead speed was set to 1 mm/min during testing.[32,33]

Printing parameters used in single-material and multi-material MMVPP experiments are depicted in Table 2.

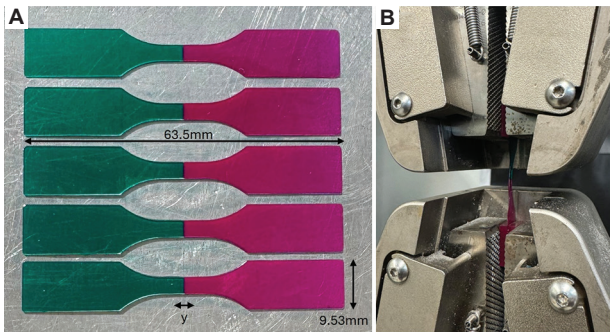


**Figure 10.** Tensile testing of multi-material printing. (A) Multi-material vat photopolymerization-printed samples as per ASTM D638–22 standard; (B) Tensile testing of the multi-material sample

## 3. Results

### 3.1. Results of material boundary

Upon inspecting the printed samples shown in Figure 7, the results summarized in Table 3 represent the dimensional measurements obtained.

During printing, noticeable variations in the final sample height were observed depending on the chosen layer thickness. Samples fabricated at larger layer heights (≥0.08 mm) exhibited greater deviations from the nominal design height, likely due to cumulative errors in resin recoating and layer adhesion during multi-material switching. Conversely, as the layer height decreased, the printed parts demonstrated improved dimensional fidelity.

It was observed that the system maintained reliable performance down to a minimum layer height of 0.035 mm, beyond which printing instability or incomplete curing occurred, which correlates with the layer height of commercially available printing technologies.[34] At this smallest tested layer height, the deviation between designed and printed height was minimal, confirming enhanced accuracy under finer layer heights.

These findings indicate that smaller layer heights not only improve vertical resolution but also mitigate cumulative shrinkage and interfacial mismatch errors between material transitions. Thus, lower layer heights represent optimal parameters for achieving dimensional consistency in dual material photopolymerization.

The observed deviations arise primarily from the increased vat-switching height during two-material printing. In single-material printing, the build plate rises only to the clearance level (~6 mm) to allow resin recoating under gravity. However, during material switching, the plate must rise significantly higher (set to 100 mm in this study) to clear the vats and enable replacement. This extended vertical travel introduces linearity errors when reinitializing printing with the second material.[35]

**Table 2. Printing parameters of single-material and multi-material MMVPP experiments**

| Parameter (unit) | Monolithic specimen | No-overlap specimen | Overlapped specimen |
|---|---|---|---|
| Layer thickness (mm) | 0.1 | 0.1 | 0.1 |
| Initial exposure time (seconds) | 40 | 40 | 40 |
| Layer exposure time (seconds) | 3 | 3 | 3 |
| Number of materials | 1 | 2 | 2 |
| Lifting height (mm) | 60 | 100 | 100 |
| Cleaning method | Not cleaned | Manual | Manual |
| Overlap length (mm) | Not applicable | 0 | 1 |

**Table 3. Sample height variation with the change of layer height**

| Layer height (mm) | Switching layer | Sample height (mm) |
|---|---|---|
| 0.05 (reference) | - | 9.94 |
| 0.100 | 45 | 7.81 |
| 0.080 | 56 | 8.23 |
| 0.070 | 64 | 8.56 |
| 0.060 | 75 | 8.62 |
| 0.050 | 90 | 8.85 |
| 0.045 | 100 | 8.87 |
| 0.035 | 128 | 8.93 |

### 3.2. Results of testing for mechanical properties at the interface

The tensile behavior of the three specimen configurations—monolithic, no-overlap, and 1 mm overlap—fabricated via MMVPP is presented in Figure 11. Distinct differences in stress–strain response were observed as a function of interfacial design.

The monolithic specimen exhibited the highest overall tensile performance, with a gradual strain-hardening response leading to an ultimate stress of 64.22 MPa at an elongation of 0.9 mm. This specimen maintained a stable load-bearing capacity throughout deformation, indicative of a homogeneous material system without interfacial discontinuities.

The 1 mm overlap specimen demonstrated mechanical behavior closely approaching that of the monolithic specimen. Its curve revealed a continuous increase in stress, achieving an ultimate value of 59.30 MPa at 0.85 mm elongation. The similarity in stress–strain response at

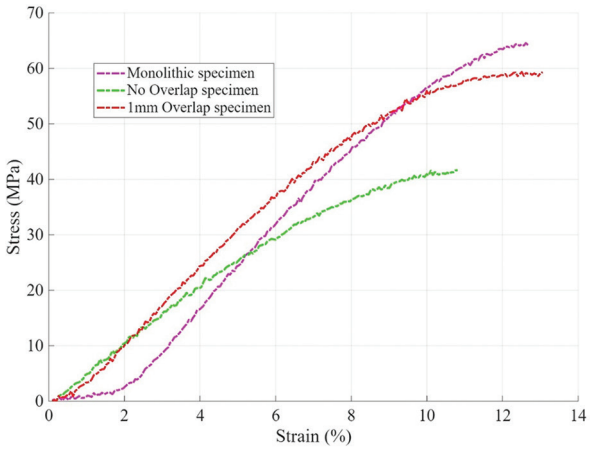


**Figure 11.** Stress–strain responses of monolithic, no-overlap multi-material, and 1 mm overlap multi-material specimens under tensile loading

higher deformation levels suggests that the introduction of a 1 mm overlap effectively facilitated stress transfer across the material interface, thereby mitigating potential weaknesses typically associated with multi-material joints.

In contrast, the no-overlap specimen displayed markedly inferior tensile properties. The stress plateaued at 41.34 MPa, with limited strain hardening and an earlier onset of failure relative to the other two configurations. This reduction in mechanical performance is attributed to insufficient interfacial bonding, which restricted load transfer and promoted premature failure.

Collectively, these findings highlight the critical role of interfacial architecture in governing the tensile response of MMVPP specimens. The inclusion of a modest overlap significantly enhanced tensile strength and ductility compared to the no-overlap configuration, producing behavior more closely aligned with that of the monolithic control.

When accounting for the material configuration, as shown in Figure 12, the boxplot reveals a clear divergence in interface behavior in two-material samples with overlapping versus non-overlapping configurations. For the two-material non-overlapping (overlap length 0 mm), the low median peak stress (41.03 MPa) and relatively large scatter indicate that failure is controlled by a weak, discontinuous interface, where stress concentrations and imperfect interfacial bonding dominate load transfer. Introducing a 1.00 mm overlap in the two-material samples leads to a sharp increase in median peak stress to 59.06 MPa and a marked reduction in variability, showing that even a small overlap is sufficient to significantly improve inter-material load transfer and mitigate interfacial stress concentrations. Notably, the peak stress of the overlapped two-material samples nearly matches that of the single-material solid samples (median 59.27 MPa), demonstrating that an adequate overlap effectively eliminates the mechanical penalty associated with a material interface. The solid samples show only a marginal increase in maximum stress, confirming that once sufficient overlap is introduced, failure is governed primarily by the intrinsic bulk material strength rather than by the presence of a material junction.

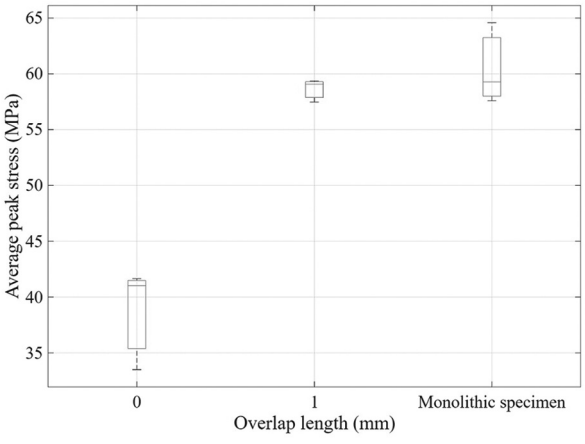


**Figure 12.** Average peak tensile stress of multi-material specimens with different overlap lengths compared to monolithic specimens.

## 4. Discussion

### 4.1. Conceptualization

The developed MMVPP platform demonstrates a conceptualized implementation of multi-resin processing with precise optical and mechanical control. The system, constructed around a 3 × 3 modular vat array, a coordinated three-axis motion build platform, and a single LED-based masking display with UV projection source, enables sequential fabrication of multi-material structures without requiring multiple curing modules. The conceptualized system enables rapid resin switching and high-resolution printing within a compact and scalable architecture.

Each vat in the array is designed with a shallow resin depth of <4 mm to reduce waste, minimize contamination with uncured resin during transfer, and maintain clear material interfaces. The build platform provides vertical motion for layer curing and lateral translation for positioning above selected vats. This controlled motion ensures alignment consistency and precise registration between different resin regions, critical for realizing multi-material features within a single component.

To address cross-contamination challenges during resin transitions, the system incorporates an integrated ultrasonic cleaning and air-blowing station adjacent to the vat array. Submersion in isopropyl alcohol with ultrasonic agitation effectively removes residual resin,[26,36,37] while a controlled air stream eliminates solvent traces before immersion in the next vat. The compact combination of cleaning and drying functions reduces both footprint and cycle time, supporting a more automated and reliable workflow for sequential resin processing. It has been proven that the ultrasonic cleaning is more effective than cleaning with a sponge or a centrifugal force.[21,24]

The present concept demonstrates that multi-material fabrication can be achieved using a single projection and motion system without compromising optical uniformity or lateral accuracy. Consistent exposure performance across vats confirms that high-resolution imaging can be maintained even when switching between photopolymers with differing viscosities and photo-sensitivities.

Future work should focus on extending this conceptual framework toward higher automation and adaptive control. Integration of closed-loop calibration for curing depth, automated resin refill and exchange mechanisms, and improved interface cleaning could further enhance throughput and material fidelity. The modular vat configuration also provides a foundation for scaling to larger arrays or integrating gradient transition components. Overall, this system establishes a practical pathway toward scalable, high-precision MMVPP.

### 4.2. Prototype development

The developed prototype was designed to demonstrate the feasibility of an MMVPP process using a modified commercial printer as a foundation. The primary goal was to transform a conventional single-material printer into a system capable of handling multiple resins with precise positioning and reliable material transitions, without compromising printing accuracy or optical quality.

The prototype modifies a commercial VPP printer to enable controlled horizontal movement of the build plate between two resin vats, allowing sequential multi-material printing. A linear rail and stepper motor ensure precise, stable motion and alignment. This approach demonstrates that multi-material fabrication can be achieved through simple mechanical and motion control upgrades rather than complex new hardware, while maintaining consistent optical exposure conditions. Automated cleaning and drying systems were not included in this design.

Experimentally, the prototype successfully produced two printed samples with clear boundaries between regions. These results confirm that the modified system can manage resin changes with minimal contamination and sufficient adhesion between successive material layers. The build process remained stable throughout printing, and no significant misalignment or structural defects were observed at the material interfaces. Furthermore, the operation of the modified printer remained consistent with that of the base system, demonstrating that the added mechanical complexity did not compromise the overall print quality.

Overall, the prototype development validates the underlying concept of MMVPP by proving that multiple materials can be processed in a controlled and repeatable manner using a compact system. The results highlight that multi-material fabrication can be achieved without complex optical realignment or multiple light sources, provided that precise mechanical motion and accurate control of resin exposure are maintained. This prototype, therefore, serves as an effective experimental platform for studying material interface quality, process timing, and layer consistency in future MMVPP systems.

### 4.3. Testing

The present study introduces and validates a framework for MMVPP, focusing on exposure control, resin switching, and interfacial reinforcement strategies. A central challenge in MMVPP is the introduction of mechanical and dimensional errors when multiple materials are cured within the same layer. The proposed offset-layer strategy effectively minimized these errors by compensating for vat deformation during material exchange. Although this approach inherently produces minor offsets between successive layers, these deviations were negligible relative to the overall part dimensions, aligning with tolerances commonly reported in AM processes.

A critical advancement of this work is the demonstration of interfacial overlap as a design parameter for enhancing mechanical performance. Tensile testing revealed that overlapped interfaces (1 mm) achieved stress–strain responses approaching those of monolithic controls, in stark contrast to non-overlapped boundaries, which exhibited premature failure and reduced load transfer. These findings underscore the importance of interfacial architecture in MMVPP, suggesting that overlap strategies significantly improve interfacial bonding by increasing the contact area across both vertical and horizontal planes. Such results echo principles of composite material design, where interfacial tailoring is critical to achieving mechanical integrity.

The influence of layer height and exposure conditions on dimensional fidelity was also apparent. Samples fabricated with lower layer heights exhibited minimal dimensional deviation, whereas greater layer heights contributed to increased shrinkage and reduced overall part height. This observation highlights the inherent trade-off between build efficiency and dimensional accuracy, a balance that must be carefully managed in practical MMVPP applications.

From a methodological standpoint, the resin switching procedure introduced additional complexity. The requirement for increased build plate clearance during vat exchange induced linearity errors, reflecting a limitation in current hardware configurations. These challenges lead to a broader need for integrated multi-resin delivery systems capable of minimizing displacement during material transitions. Future developments in vat design, such as segmented vats or automated resin feed systems, may provide pathways to mitigate this limitation.

Collectively, the results presented here establish a foundation for the controlled fabrication of multi-material

photopolymer components with tunable interfacial properties. The successful implementation of overlap-based bonding strategies demonstrates a practical means to bridge the performance gap between monolithic and multi-material prints. Nonetheless, further investigation into long-term stability, fatigue resistance, and the influence of resin chemistries will be necessary to validate the broader applicability of MMVPP for functional, load-bearing applications.

### 4.4. Limitations

Nevertheless, some challenges remain. Ultrasonic cleaning, while highly effective, may induce mechanical stresses on fragile or fine-featured prints, and optimization of frequency and exposure time will be critical for ensuring broad material compatibility. In addition, although isopropyl alcohol is widely used due to its effectiveness, future iterations may consider solvent alternatives or closed-loop recycling systems to improve sustainability and reduce solvent consumption.

During the testing, it was revealed that the linearity error induced with mechanical actuation is significant when switching the resins. To mitigate this issue, it is recommended that a high-precision rotary encoder be implemented in all motion systems requiring feedback for 3D navigation. In addition, an error-compensation algorithm should be incorporated into the control software to correct residual inaccuracies. The experiment also provided valuable insight that reducing the layer height results in lower induced linearity error.

In the present study, experimental validation was limited to single-direction printing and two-material combinations to enable systematic investigation of resin switching, exposure control, and interfacial behavior. Extension to multidirectional printing and a broader range of material mixtures will be pursued in future work.

### 4.5. Implications and application outlook

The compact MMVPP platform developed in this study enables precise multi-material control with enhanced interfacial integrity, making it suitable for several niche application domains. The demonstrated intra-layer exposure control and overlap-based interface reinforcement provide a practical route for fabricating functionally graded components, where localized property transitions are required to reduce stress concentrations or tailor mechanical response.[2]

The proposed process is also directly applicable to lattice and metamaterial architectures, including interpenetrating or aperiodic lattices, where voxel-level material placement and robust interfaces are critical for achieving enhanced mechanical performance. In such structures, interface reinforcement at strut junctions and material boundaries is particularly advantageous.[38]

In biomedical and bioinspired applications, the ability to spatially vary material properties supports the fabrication of multi-material scaffolds that better emulate natural tissue interfaces. Similarly, soft robotics and compliant mechanisms can benefit from reliable integration of mechanically dissimilar regions to enable controlled deformation without interfacial failure.[5,6,39]

Finally, the compact footprint, low resin volume, and single-projection architecture make the system well-suited for research-scale prototyping, material development, and exploratory studies of multi-material interfaces. Overall, while this work focuses on process validation, the MMVPP framework provides a versatile foundation for advanced multi-material AM in specialized applications.

## 5. Conclusion

This work establishes a practical and scalable pathway to true MMVPP by unifying curing across multiple vats with a single projection source. The conceptual MMVPP architecture supports various configurations of vat grids with minimal modification, combining shallow, low-volume vats, precise Z and X–Y motion of the build platform, and an adjacent, integrated ultrasonic cleaning and air-drying station. Using a single monochrome LCD masking display, the system maintains consistent lateral resolution and simplifies exposure calibration across resins with disparate optical and rheological properties, enabling rapid material exchange without sacrificing optical fidelity.

The developed prototype, built on a modified commercial printer, validated the feasibility of sequential multi-resin processing with reliable positioning, clean material transitions, and uniform exposure from a single light source. Two-material prints exhibited clear boundaries and adequate adhesion, confirming that controlled mechanical motion and exposure management can deliver multi-material parts without complex optical realignment or multiple curing modules.

Process strategies introduced in this study directly reinforce part integrity. An offset-layer approach constrained cumulative positional errors within typical AM tolerances during resin switching. Crucially, multi-material interfacial overlap enhances tensile performance. These results highlight interfacial architecture as a decisive design parameter for mechanical reliability in MMVPP and underscore the trade-offs between build efficiency and dimensional accuracy, particularly at greater layer heights.

Overall, the presented system and results demonstrate

that compact, unified MMVPP platforms can produce multi-material photopolymer components with controlled interfaces and consistent dimensional accuracy. Future work will extend mechanical characterization to fatigue, creep, and environmental stability; broaden resin chemistries; refine motion and switching mechanisms to further suppress induced errors; and enhance cleaning sustainability and automation. These advancements will accelerate the translation of MMVPP toward reliable manufacturing of functionally graded and composite photopolymer parts.

## Acknowledgments

None.

## Funding

This work was funded by the Academy of Finland Flagship Programme PREIN (Decision no. 320167).

## Conflict of interest

The authors declare they have no competing interests.

## Author contributions

*Conceptualization:* Wudith W. Niyagama, Jouni Partanen
*Funding acquisition:* Jouni Partanen
*Investigation:* Wudith W. Niyagama, S. Siddharth Kumar
*Methodology:* Wudith W. Niyagama
*Project administration:* Jouni Partanen
*Supervision:* Tuomas Puttonen
*Validation:* Tuomas Puttonen
*Visualization:* S. Siddharth Kumar
*Writing–original draft:* Wudith W. Niyagama
*Writing–review & editing:* S. Siddharth Kumar, Tuomas Puttonen

## Ethics approval and consent to participate

Not applicable.

## Consent for publication

Not applicable.

## Availability of data

Data are available from the corresponding author upon reasonable request.

## References

1. Gibson I. *Additive Manufacturing Technologies*. 3rd ed. Germany: Springer; 2021.

2. Loh GH, Pei E, Harrison D, Monzón MD. An overview of functionally graded additive manufacturing. *Addit Manuf*. 2018;23:34-44.
doi: 10.1016/j.addma.2018.06.023

3. Subedi S, Liu S, Wang W, Naser Shovon SMA, Chen X, Ware HOT. Multi-material vat photopolymerization 3D printing: A review of mechanisms and applications. *Npj Adv Manuf*. 2024;1(1):9.
doi: 10.1038/s44334-024-00005-w

4. Sampson KL, Deore B, Go A, *et al*. Multimaterial vat polymerization additive manufacturing. *ACS Appl Polym Mater*. 2021;3(9):4304-4324.
doi: 10.1021/acsapm.1c00262

5. Nazir A, Gokcekaya O, Md Masum Billah K, *et al*. Multi-material additive manufacturing: A systematic review of design, properties, applications, challenges, and 3D printing of materials and cellular metamaterials. *Mater Des*. 2023;226:111661.
doi: 10.1016/j.matdes.2023.111661

6. Salmi M. Additive manufacturing processes in medical applications. *Materials*. 2021;14(1):191.
doi: 10.3390/ma14010191

7. Kumar SS, Akmal JS, Salmi M. 4D printing of shape memory polymer with continuous carbon fiber. *Prog Addit Manuf*. 2024;9(6):1985-1995.
doi: 10.1007/s40964-023-00553-1

8. Kumar SS, Niyagama WW, Akmal JS, Salmi M. 4D printing of electro-activated thermochromic composites for dynamic 3D displays. *Mater Des*. 2025;251:113674.
doi: 10.1016/j.matdes.2025.113674

9. Ghaderi I, Behravesh AH, Hedayati SK, *et al*. Multimaterial additive manufacturing of poly-L-lactic acid–hydroxylapatite/graphene oxide scaffold fabricated via vat photopolymerization: Experimental investigation, analysis and cell study. *Rapid Prototyp J*. 2024;30(9):1789-1802.
doi: 10.1108/RPJ-02-2024-0085

10. Al Rashid A, Ahmed W, Khalid MY, Koç M. Vat photopolymerization of polymers and polymer composites: Processes and applications. *Addit Manuf*. 2021;47:102279.
doi: 10.1016/j.addma.2021.102279

11. McKerricher G, Vaseem M, Shamim A. Fully inkjet-printed microwave passive electronics. *Microsyst Nanoeng*. 2017;3(1):16075.
doi: 10.1038/micronano.2016.75

12. Vyas A, Garg V, Ghosh SB, Bandyopadhyay-Ghosh S. Photopolymerizable resin-based 3D printed biomedical composites: Factors affecting resin viscosity. *Mater Today Proc*. 2022;62:1435-1439.
doi: 10.1016/j.matpr.2022.01.172

13. Choi JW, Kim HC, Wicker R. Multi-material stereolithography. *J Mater Process Technol*. 2011;211(3):318-328.

doi: 10.1016/j.jmatprotec.2010.10.003

14. Inamdar A, Magana M, Medina F, Grajeda Y, Wicker R. Development of an automated multiple material stereolithography machine. In: *17th Annual International Solid Freeform Fabrication (SFF) Symposium in Austin TX*. 2006. p. 624-635.

15. Wicker R, Medina F, Elkins C. Multiple material micro-fabrication: Extending stereolithography to tissue engineering and other novel applications. In: *15th Annual International Solid Freeform Fabrication (SFF) Symposium in Austin TX*. 2004. p. 754-764.

16. Zhou C, Chen Y, Yang Z, Khoshnevis B. Digital material fabrication using mask-image-projection-based stereolithography. *Rapid Prototyp J*. 2013;19(3):153-165.

doi: 10.1108/13552541311312148

17. Huang P, Deng D, Chen Y. Modeling and fabrication of heterogeneous three-dimensional objects based on additive manufacturing. In: *Volume 2A: Advanced Manufacturing*. United States: American Society of Mechanical Engineers; 2013. p. V02AT02A056.

doi: 10.1115/IMECE2013-65724

18. Bhusal A, Dogan E, Nguyen HA, *et al*. Multi-material digital light processing bioprinting of hydrogel-based microfluidic chips. *Biofabrication*. 2022;14(1):014103.

doi: 10.1088/1758-5090/ac2d78

19. Jiang CP, Romario YS, Bhat C, Hentihu MFR, Zeng XC, Ramezani M. Design and fabrication of multi-material pneumatic soft gripper using newly developed high-speed multi-material vat photopolymerization 3D printer. *Int J Adv Manuf Technol*. 2024;130(3-4):1093-1106.

doi: 10.1007/s00170-023-12774-3

20. Matte CD, Pearson M, Trottier-Cournoyer F, Dafoe A, Kwok TH. Automated storage and active cleaning for multi-material digital-light-processing printer. *Rapid Prototyp J*. 2019;25(5):864-874.

doi: 10.1108/RPJ-08-2018-0211

21. Shaukat U, Thalhamer A, Rossegger E, Schlögl S. Dual-vat photopolymerization 3D printing of vitrimers. *Addit Manuf*. 2024;79:103930.

doi: 10.1016/j.addma.2023.103930

22. Khatri B, Frey M, Raouf-Fahmy A, Scharla MV, Hanemann T. Development of a multi-material stereolithography 3D printing device. *Micromachines*. 2020;11(5):532.

doi: 10.3390/mi11050532

23. Hu K, Zhao P, Li J, Lu Z. High-resolution multiceramic additive manufacturing based on digital light processing. *Addit Manuf*. 2022;54:102732.

doi: 10.1016/j.addma.2022.102732

24. Cheng J, Wang R, Sun Z, *et al*. Centrifugal multimaterial 3D printing of multifunctional heterogeneous objects. *Nat Commun*. 2022;13(1):7931.

doi: 10.1038/s41467-022-35622-6

25. Wu X, Lian Q, Li D, Jin Z. Biphasic osteochondral scaffold fabrication using multi-material mask projection stereolithography. *Rapid Prototyp J*. 2019;25(2):277-288.

doi: 10.1108/RPJ-07-2017-0144

26. Nam OH, Chung SY, Hyun HK, *et al*. Influence of postprinting cleaning methods on the cleaning efficiency and surface and mechanical properties of three-dimensionally printed resins. *J Prosthet Dent*. 2024;132(4):838.e1-838.e9.

doi: 10.1016/j.prosdent.2024.02.026

27. Parks GS, Barton B. Vapor pressure data for isopropyl alcohol and tertiary butyl alcohol. *J Am Chem Soc*. 1928;50(1):24-26.

doi: 10.1021/ja01388a004

28. Santos EO, Oliveira PLE, De Mello TP, *et al*. Surface characteristics and microbiological analysis of a vat-photopolymerization additive-manufacturing dental resin. *Materials*. 2022;15(2):425.

doi: 10.3390/ma15020425

29. ASTM Subcommittee D20. *Standard Test Method for Tensile Properties of Plastics*. United States: ASTM International; 2022.

doi: 10.1520/D0638-22

30. Riccio C, Civera M, Grimaldo Ruiz O, *et al*. Effects of curing on photosensitive resins in SLA additive manufacturing. *Appl Mech*. 2021;2(4):942-955.

doi: 10.3390/applmech2040055

31. Anastasio R, Peerbooms W, Cardinaels R, van Breemen LCA. Characterization of ultraviolet-cured methacrylate networks: From photopolymerization to ultimate mechanical properties. *Macromolecules*. 2019;52(23):9220-9231.

doi: 10.1021/acs.macromol.9b01439

32. Ligon SC, Liska R, Stampfl J, Gurr M, Mülhaupt R. Polymers for 3D printing and customized additive manufacturing. *Chem Rev*. 2017;117(15):10212-10290.

doi: 10.1021/acs.chemrev.7b00074

33. Wang X, Jiang M, Zhou Z, Gou J, Hui D. 3D printing of polymer matrix composites: A review and prospective. *Compos Part B Eng*. 2017;110:442-458.

doi: 10.1016/j.compositesb.2016.11.034

34. Pagac M, Hajnys J, Ma QP, *et al*. A Review of vat photopolymerization technology: Materials, applications, challenges, and future trends of 3D printing. *Polymers*. 2021;13(4):598.

doi: 10.3390/polym13040598

35. Lur'e ZY. Analysis of pitch error in lead screws. *Meas Tech*. 1973;16(9):1340-1341.

doi: 10.1007/BF00813042

36. Jin G, Gu H, Jang M, *et al*. Influence of postwashing process on the elution of residual monomers, degree of conversion, and mechanical properties of a 3D printed crown and bridge materials. *Dent Mater*. 2022;38(11):1812-1825.

doi: 10.1016/j.dental.2022.09.017

37. Hassanpour M, Narongdej P, Alterman N, Moghtadernejad S, Barjasteh E. Effects of post-processing parameters on 3D-printed dental appliances: A review. *Polymers*. 2024;16(19):2795.

doi: 10.3390/polym16192795

38. Wang X, Li Z, Deng J, *et al*. Unprecedented strength enhancement observed in interpenetrating phase composites of aperiodic lattice metamaterials. *Adv Funct Mater*. 2025;35(1):2406890.

doi: 10.1002/adfm.202406890

39. Xavier MS, Tawk CD, Yong YK, Fleming AJ. 3D-printed omnidirectional soft pneumatic actuators: Design, modeling and characterization. *Sens Actuators Phys*. 2021;332:113199.

doi: 10.1016/j.sna.2021.113199

## Appendix

Schematic of the control architecture of a multi-material vat photopolymerization system